

Characterization of THz-induced bias voltage modulation in an STM

Yang Luo¹, Jesus A. M. Calzada¹, Gong Chen^{2,3}, Peter H. Nguyen¹, Vedran Jelic^{1,4}, Yu-Jui Ray Liu¹, Daniel J. Mildenberger¹, Howe R. J. Simpson¹, and Frank A. Hegmann¹

¹Department of Physics, University of Alberta, Edmonton, Alberta T6G 2E1, Canada

²School of Physics and Engineering, Zhengzhou University, Zhengzhou 450052, China

³Hefei National Laboratory for Physical Sciences at the Microscale and Synergetic Innovation Center of Quantum Information & Quantum Physics, University of Science and Technology of China, Hefei, Anhui 230026, China

⁴Current address: Department of Physics and Astronomy, Michigan State University, East Lansing, Michigan 48824, USA

Abstract—To understand and characterize the transient bias voltage induced by single-cycle terahertz (THz) pulses coupled to a scanning tunneling microscope (STM), the Bardeen tunneling model is applied to a 3-dimensional geometry of the STM junction. The simulated THz-induced tunneling current at the junction agrees well with that observed by THz-STM on a Cu(111) surface, providing a benchmark to quantify the THz-induced bias voltage at the tip-sample interface.

I. INTRODUCTION

Ultrafast single-cycle terahertz pulses coupled to a scanning tunneling microscope (THz-STM) can provide simultaneously sub-nanometer spatial resolution and sub-picosecond temporal resolution [1–5]. The localized transient terahertz fields modulate the bias voltage at the tunnel junction allowing the investigation of ultrafast dynamics at the nanoscale.

Simulations to explain THz-STM results have been reported for doped silicon surfaces [3] and single pentacene molecules [4], and terahertz near-fields have been studied [5,6]. However, in general, a comparison between conventional STM and THz-STM tunneling currents cannot be done directly because the latter requires either larger transient voltages or significantly lower tip-sample distances. Thus, our model approach aims to expand the steady-state tunneling theory to simulate the THz-induced transient tunneling current.

A metal tip on a metal surface offers a basic system with well-known density of states to understand the THz-induced currents at the STM junction. The Bardeen tunneling model with a three-dimensional geometry of the tip-sample junction was used for our simulations. With a semiclassical approach, the tunnel current was calculated by integrating the local current density over the tip surface, which consists of a 10 nm radius sphere with a small protrusion at the apex represented by a 1 nm sphere, as shown in Fig. 1a.

II. RESULTS

The Bardeen tunneling model was used to simulate the THz induced tunneling current (I_{THz}) based on steady-state tunneling theories and a three-dimensional geometry for the tip and sample. This approach allowed us to calculate the THz-induced bias voltage at the STM junction, which suggests high THz-induced peak bias voltages ranging from 7 V to 14 V. These THz-induced voltages are larger than the work function of the tip and the sample, which suggests that the THz-induced currents were generated in the field emission regime.

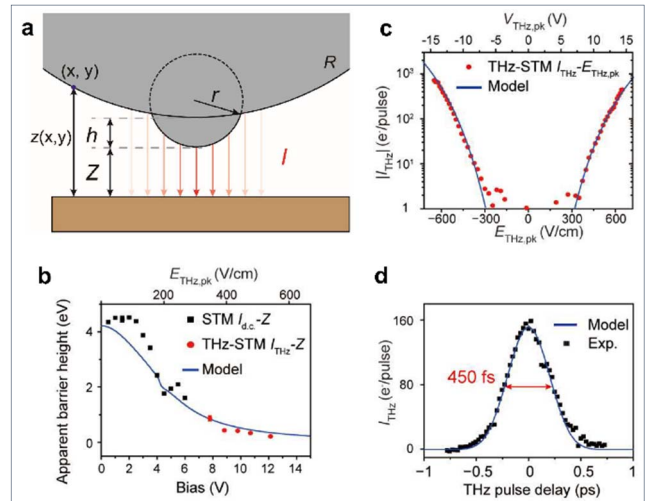


Fig. 1. (a) Cross-section of the 3D tunnel junction, with the STM tip modeled by two spheres of radius R and r . (b) Apparent barrier heights obtained experimentally for steady-state STM (black dots) and THz-STM (red dots) and the values calculated from our model (blue solid line). (c) THz-STM $I_{\text{THz}} - E_{\text{Thz},\text{pk}}$ curves ($V_{\text{dc}} = 0.1$ V) from the experiment (red dots) and simulations (blue solid line). (d) Autocorrelation measurement for the experimental (black dots) and calculated (blue solid line) I_{THz} as a function of overlap time.

Apparent barrier heights (ABHs) extracted from the exponential decay of the STM I_{dc}, Z curves decrease rapidly when the bias voltage is near the work function of the tip and sample due to an increase in the tunneling probability. The ABHs for the THz-induced current obtained from the I_{THz}, Z curves are even lower, corresponding to high THz-induced bias voltages and therefore confirming the THz-STM is operating in the field emission regime. The ABH as a function of bias voltage for STM and THz-STM is shown in Fig. 1b.

The experimentally measured THz-STM $I_{\text{THz}} - E_{\text{Thz},\text{pk}}$ curves were accurately reproduced by our simulations, as shown in Fig. 1c. An autocorrelation measurement of the THz pulse was used to determine the temporal resolution of the THz-STM on the Cu(111) surface. A full width at half maximum (FWHM) of 450 fs was obtained experimentally and a similar value was produced by our simulations, as can be seen in Fig. 1d. The good agreement between the experimental and calculated data, suggests that our model was able to represent the tunneling processes at both the low-voltage and high-voltage ranges.

Furthermore, a scaling factor (S) of $S=1/45$ cm was obtained from the simulation, which corresponds to a field enhancement factor (F) of $F \approx 2.2 \times 10^5$ for the incident THz pulse electric field, which is similar to the value obtained in Ref. [3].

High THz-induced bias voltages translate into a larger tunneling area compared to a low d.c. bias in a steady-state STM. A topographic STM image and a THz-STM image, acquired simultaneously, are shown in Fig. 2a for comparison. A profile line is drawn to indicate the path of the tip over a step-edge. The linescans of the relative tip height and THz-induced tunnel current along the profile line, shown in Fig. 2b, illustrate the difference in the tunneling area. As the tip gets closer to the step edge from the upper side, the THz-induced current decreases due to a larger tunneling region, before any changes in the d.c. current are detected. Similarly, if the tip approaches the step edge from the lower side, an increase in THz-induced current is observed.

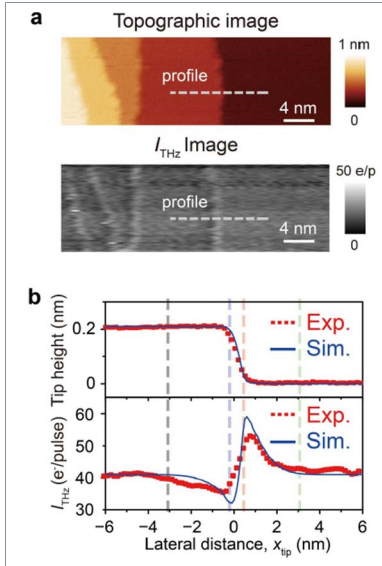


Fig. 2. (a) STM topography and THz-STM image of the Cu(111) surface simultaneously acquired. (b) Experimental (red dots) and simulated (blue solid lines) linescans along the profile line in (a) showing the relative tip height and the THz-induced tunnel current.

In terahertz-driven STM mode (TD-STM) the average THz-induced current is higher than the d.c. current and therefore dominates the current setpoint. THz-induced current images of a step-edge formed by three-atomic layers, acquired with TD-STM, suggest a lateral spatial resolution of 2 nm. STM and TD-STM images of the Cu(111) surface are shown in Fig. 3a and Fig. 3b, respectively. The linescans over a defect, a single atomic step and a three-atomic layers step are shown in Fig. 3c, Fig. 3d and Fig. 3e, respectively.

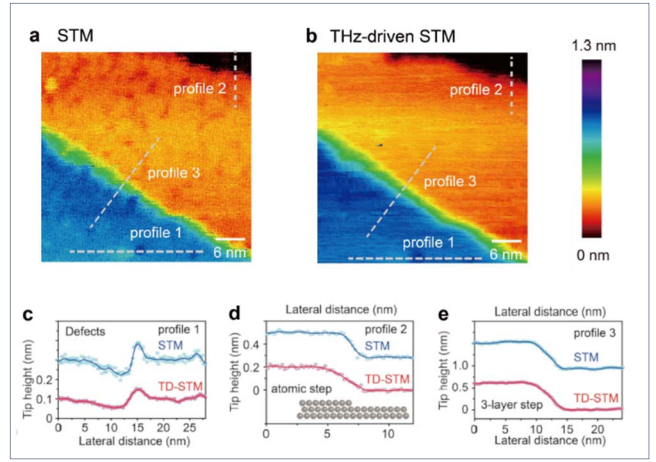


Fig. 3. (a) STM topography of the Cu(111) surface, acquired with $V_{\text{d.c.}} = 0.1$ V and $I_{\text{d.c.}} = 20$ pA. (b) THz-driven STM (TD-STM) of the same zone as (a) acquired with $E_{\text{THz,pk}} = 450$ V/cm, $I_{\text{d.c.}} + I_{\text{THz,avg}} = 20$ pA, $V_{\text{d.c.}} = 0.1$ V. (c) (d) (e) Linescans along the gray dashed lines in (a) and (b), displaying the spatial resolution of STM and TD-STM over a defect, a single atomic step and a three-atomic layers step, respectively.

III. SUMMARY

The simulations based on a 3D tip-sample model are in good agreement with the experimentally observed THz-induced tunnel currents and were used to quantify the transient THz-induced bias voltage at the STM junction. The model was able to reproduce the tunneling processes at both the low-voltage and high-voltage ranges. This model is important for understanding THz-STM imaging of nanoscale features on metal surfaces.

This work was supported by the Natural Sciences and Engineering Research Council of Canada (NSERC), the Canada Foundation for Innovation (CFI), and the Alberta Innovates Technology Futures (AITF) Strategic Chairs Program. We are grateful for technical support from Greg Popowich, James Chaulk and Beipei Shi.

REFERENCES

- [1] T. L. Cocker, V. Jelic, M. Gupta, S. J. Molesky, J. A. J. Burgess, G. De Los Reyes, L. V. Titova, Y. Y. Tsui, M. R. Freeman, and F. A. Hegmann, "An ultrafast terahertz scanning tunnelling microscope," *Nat. Photon.* 7, 620 (2013).
- [2] K. Yoshioka, I. Katayama, Y. Minami, M. Kitajima, S. Yoshida, H. Shigekawa, and J. Takeda, "Real-space coherent manipulation of electrons in a single tunnel junction by single-cycle terahertz electric fields," *Nat. Photon.* 10, 762 (2016).
- [3] V. Jelic, K. Iwaszczuk, P. H. Nguyen, C. Rathje, G. J. Hornig, H. M. Sharum, J. R. Hoffman, M. R. Freeman, and F. A. Hegmann, "Ultrafast terahertz control of extreme tunnel currents through single atoms on a silicon surface," *Nat. Phys.* 13, 591 (2017).
- [4] T. L. Cocker, D. Peller, P. Yu, J. Repp, and R. Huber, "Tracking the ultrafast motion of a single molecule by femtosecond orbital imaging," *Nature* 539, 263 (2016).
- [5] S. Yoshida, H. Hirori, T. Tachizaki, K. Yoshioka, Y. Arashida, Z.-H. Wang, Y. Sanari, O. Takeuchi, Y. Kanemitsu, and H. Shigekawa, "Subcycle transient scanning tunneling spectroscopy with visualization of enhanced terahertz near field," *ACS Photonics.* 6 (6), 1356-1364 (2019).
- [6] M. Müller, N. Martín Sabanés, T. Kampfrath and M. Wolf, "Phase-Resolved Detection of Ultrabroadband THz Pulses inside a Scanning Tunneling Microscope Junction," *ACS Photonics.* 7 (8), 2046-2055 (2020).